SIMULATION SUPPORTED PROFILE RECONSTRUCTION WITH MACHINE LEARNING

R. Singh, M. Sapinski and D. Vilsmeier, GSI, Darmstadt, Germany

Abstract

Measured IPM profiles can be significantly distorted due to displacement of residual ions or electrons by interaction with beam fields for high brightness or high energy beams [1–6]. It is thus difficult to deduce the characteristics of the actual beam profile from the measurements. Artificial neural network with multilayer perceptron (ANN-MLP) architecture is applied to reconstruct the actual beam profile from the measurement data. The MLP is trained using Virtual-IPM simulation program [7] developed under the IPMSim collaboration [8]. The first results are presented in this contribution.

INTRODUCTION

Ionization Profile Monitors (IPM) are used for non-destructive transverse beam profile measurements at many accelerator facilities. The principle of operation is the following; the primary beam ionizes the residual gas and the ionized particles (ions or electrons) are extracted via electric fields and sometimes in conjunction with magnetic fields to confine the movement of ionized particles in the plane transverse to the electric field. The profile of the extracted particles reflects the transverse profile of the primary beam with the assumption that ionized particles are created at rest and the effect of induced fields by the primary beam on ionized particles can be neglected. The choice between ions or electrons for profile reconstruction is based on the requirement for the speed of device operation and potential influence of beam space charge.

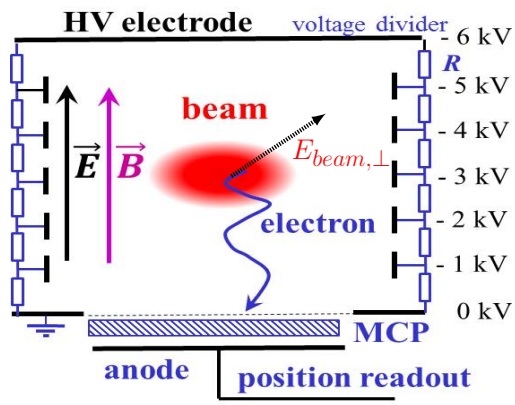

Figure 1: Operating principle of the IPM.

Figure 1 shows the typical components present in an IPM where both the electric and magnetic fields are utilized to confine the ionized particles [9]. The support electrodes/rods between the top and bottom electrodes are used to reduce the fringe fields and improve field homogeneity. The field homogeneity is important in order to avoid any distortion in the measured profile and therefore static EM simulations for the full geometry are usually performed. IPMs are often used for non-destructive measurements in low pressure conditions such as storage rings and hence they usually have to be equipped with a high amplification multi-channel plate (MCP) for obtaining sufficient signal to noise ratio. The output of MCPs are connected to data acquisition system directly or via phosphor screens and optical system. Figure 2 shows the image of the horizontal IPM formerly installed at LHC relevant to the discussions in this paper [4]. The dipole magnet has been moved in order to make the IPM chamber visible. In the next section, we will discuss the distortion in measured IPM profiles due to beam space charge and discuss previous efforts on correcting or reducing the distortion. Following that, the simulation tool and the beam and device parameters used to train the artificial ANN-MLP are discussed. Finally, the ANN-MLP parameters, training and validation are presented and the results are summarized.

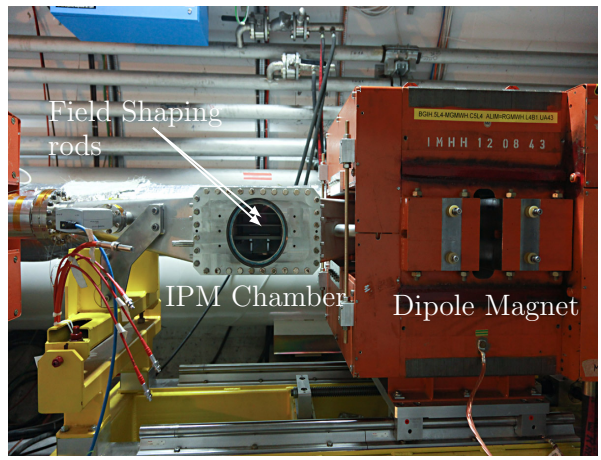

Figure 2: IPM installation at LHC. The dipole magnet (orange) has been shifted, revealing the IPM chamber.

SPACE CHARGE EFFECTS ON IPM PROFILE

IPM profile distortion due to beam fields depends on a variety of parameters such as device geometry, beam properties, extracted particle types (ions or electrons) and if IPM uses only electric field or also magnetic field. Initial IPM developments were focused around devices utilizing only electric fields. The distortion of IPM profiles has long been observed and the first attempt to make a simulation-based correction was by Thern [1] at AGS. Calculation of actual beam profile width from measured profile as a function of applied electric field and bunch population for coasting and bunched

ISBN 978-3-95450-192-2

beams was found. Further modifications were made to the Thern analytical model and were experimentally applied at FNAL [2]. Such analytical models made assumptions concerning the beam profile shape and predictions diverged for dense beams. A numerical approach was attempted at CEA Saclay during development of LIPAc IPMs, where very high space charge is expected [3]. In that correction procedure, first simulations were used to map the actual profile with the measured profile and the mapping was stored in matrices for a range of actual beam profiles modelled as generalized Gaussian distribution and for a range of beam currents. A fast iterative procedure was implemented to utilize these matrices for profile reconstruction experimentally. Practical limitations of this approach was that error in reconstructed profile was dependent on the size or coarseness of the simulation grid, and further reduction of grid size increased the number of reconstruction matrices significantly due to curse of dimensionality. Alternative approach for dealing with profile distortion is to use magnetic fields to confine the generated ionized particles around the point of generation. However, in addition to being expensive, required magnetic field strengths are prohibitory for extremely dense beams as discussed below for our target case. First major distortion for an IPM with magnetic fields was seen for LHC IPMs at high energies, where the beam profile was significantly broader compared to wire scanner measurements [4]. First solution envisaged to solve the issue was to raise the magnetic fields in the IPM to 1 T [5]. This field strength should be viewed in perspective of the strength of LHC main dipoles which is 8.5 T at top energies and is considered impractical. Following that, correction methods such as quartile and sieve method were contemplates to reconstruct the beam profile [6] but such attempts were either impractical or unsuccessful.

Recently reliable IPM simulation tools has been developed as joint effort between several labs [8]. Availability of reliable description of IPM system including the profile distorting effects such as space charge and initial velocity distribution of ionized particles transforms the problem of IPM profile correction into a "supervised learning" problem. In a supervised learning problem, the input and output of an unknown system are provided and the system is approximated with a variety of machine learning algorithms [10]. We have chosen the multi-layer perceptron architecture of artificial neural network (ANN-MLP) as a first approach to reconstruct actual beam profile from the measured distorted profile. We have also simplified the problem by assuming Gaussian primary beams for first tests presented here, however these are not limitations of the method itself and can be extended to arbitrary profiles.

VIRTUAL-IPM AND SIMULATION DATA DETAILS

The Virtual-IPM simulation program has been used in order to generate beam profiles for LHC parameters. Table 1 shows the parameters which have been used for the simulations. σ_x, σ_y, σ_l and the bunch population N_p have been varied to cover the relevant operational region. The simulation used a Gaussian bunch shape and an analytical solution for the electric field of a Gaussian bunch in two dimensions, neglecting the longitudinal field component. This is justified because the bunch is highly relativistic and is longitudinal size is significantly larger than transverse size. The initial velocities of electrons were sampled from the Voitkiv double differential cross section [11] for a Hydrogen target. Each case simulated 1×10^6 particles whose final positions were grouped into profiles with 100 µm bin size.

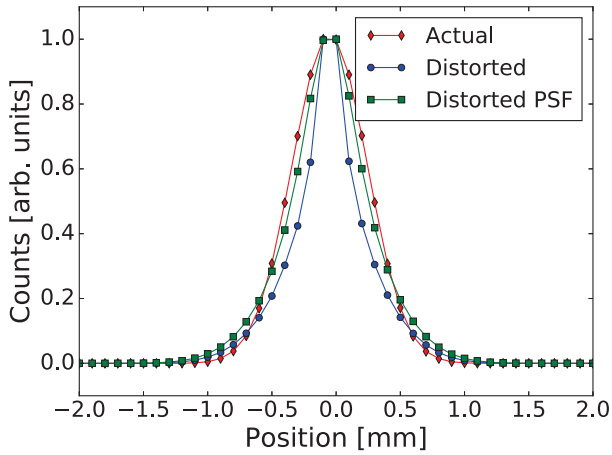

Figure 3: Simulation of profile distortion due to space charge using Virtual IPM.

Table 1: Parameters Used for the Simulation. σ_x, σ_y, σ_l and the Bunch Population Have Been Varied within the Specified Intervals.

Particle type	Protons
Energy/u	6.5 TeV
Bunch population N_p	1.1×10^{11} to 1.7×10^{11}
Bunch length σ_l (4σ)	0.9 ns to 1.2 ns
Bunch width σ_x (1σ)	0.29 mm to 0.37 mm
Bunch height σ_y (1σ)	0.4 mm to 0.6 mm
Electrode distance	85 mm
Applied voltage	4 kV
Magnetic field	0.2 T

One million particles were used in each simulation providing rather smooth profiles. The bin size is 0.1 mm and Gaussian point spread function with $\sigma = 0.125$ mm was used to represent the effect of optical acquisition system in the LHC IPM system. Figure 3 shows the actual primary beam profile, the distorted profile due to space charge and the profile read at the end of the acquisition system after application of point spread function of the optics. The input parameters to simulation were $N_p = 1.7 \times 10^{11}$, $\sigma_l = 0.9$ ns, $\sigma_x = 0.29$ mm, and $\sigma_y = 0.4$ mm . There is a 20 % increase in the second central moment of the measured profile (with PSF) with respect to actual (initial) profile.

ISBN 978-3-95450-192-2

MULTI-LAYER PERCEPTRON

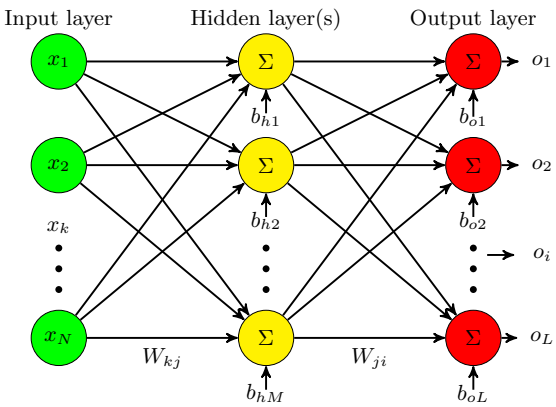

Figure 4: Schematic showing the architecture of the ANN-multilayer perceptron.

Figure 4 shows the single layer MLP, where each of the nodes in the hidden and output layer sums all the inputs and transforms them using a non-linear "activation function" g. The activation function can be any differentiable non-linear function. Typically used activation functions are "sigmoid" and "tanh". A multilayer perceptron with at least one hidden layer is known to be a universal approximator [12] and can be shown to represent any function with sufficient number of nodes. For the given training inputs x and outputs y, the hidden function is approximated by,

$$o_i = g\left(\sum_{j=1}^{M} W_{ji} \cdot g\left(\sum_{k=1}^{N} W_{kj} \cdot x_k + b_{hj}\right) + b_{oi}\right) \quad (1)$$

Weights are randomly initialized and iteratively updated in order to minimize the selected loss function,

$$E = \sum_{i=1}^{L} (y_i - o_i)^2 \quad (2)$$

A commonly used loss function is mean square error, and the gradient of the loss function with respect to network weights and biases are calculated using gradient descent method at each step and back propagated to the weights in previous layers. This full procedure is referred to as back-propagation. There are several variants for calculating the gradients during backpropagation [10].

Figure 5 shows the process of generating the training and validation data and its usage in the training of the ANN-MLP. The training data is used to optimize the weights and biases of each node in the ANN-MLP to approximate the function f' with Eq. 1 and validation data is used to check if the approximated/learned function generalizes to intermittent space within the training grid.

The training ANN-MLP is performed with three distinct parameters, measured profile (100 points in each profile),

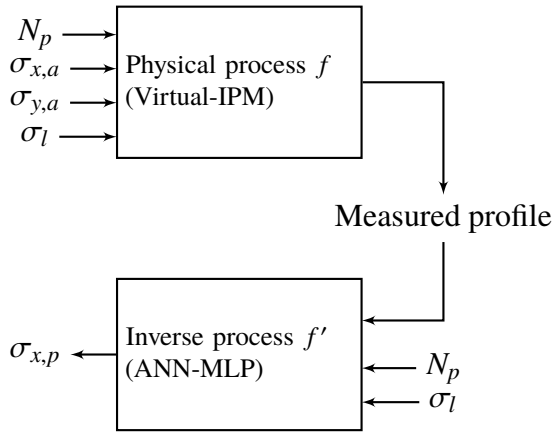

Figure 5: Physical process modelled by Virtual-IPM and the inverse process approximated by ANN-MLP.

particle number N_p (1 point) and bunch length σ_l (1 point) as inputs forming an array of 102 points for each training sample while the output is actual width denoted by $\sigma_{x,a}$ to differentiate from predicted width $\sigma_{x,p}$. $\sigma_{y,a}$ is not used for the training process since in any experimental usage, it will not be available as an input to the trained network for pre-diction of $\sigma_{x,p}$. 375 training samples were generated with a parameter scan in N_p, $\sigma_{x,a}$ and $\sigma_{y,a}$ (5 parameters each) and σ_l (3 parameters). Table 1 shows the parameter range over which training data was generated. Validation data was generated at a spacing 1 %, 25 % and 50 % off the training data sites in each parameter space forming 372 validation samples. In addition to that 0.5 % Gaussian white noise (rel-ative to the maximum value in each parameter space) was added to the profiles to depict ADC/camera noise on the measured profile as well as measurement uncertainty on N_p and σ_l. Tensorflow [13] library with Keras [14] interface was used to define and train the ANN-MLP. We have utilized two hidden layers of 60 and 30 nodes each and 1 output node in our MLP architecture. The activation function used is "tanh" and "adam" optimizer is selected for calculation of gradient of loss function with respect to MLP parameters. Training was performed in batch learning mode in batches of 4 and 200 epoches were performed. One complete training took less than a minute on a standard PC.

RESULTS AND DISCUSSION

Figure 6 shows the reconstructed beam width for the validation data by the trained ANN-MLP plotted against actual (initial) beam width. The training and validation grids are marked. Though the variation of parameters are performed in the four-dimensional parameter space, only the grid for parameter σ_x is indicated in the plot. Figure 7 shows the histogram of the percentage error of beam σ_x prediction, and a bias and variance of less than 1 % was obtained.

Robustness

The influence of measurement uncertainties on the artificial neural network training and prediction was also studied.

ISBN 978-3-95450-192-2

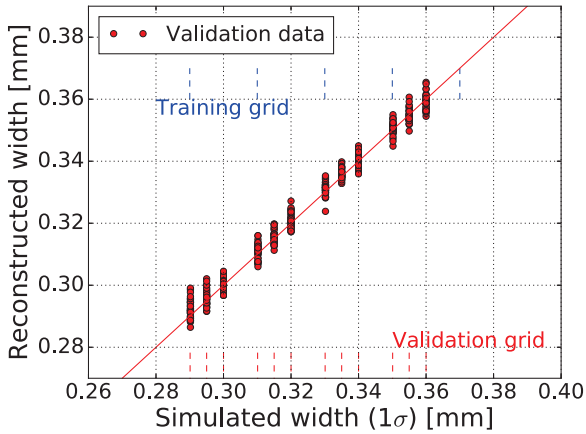

Figure 6: Prediction of actual profile width from distorted measured profile using an ANN-MLP.

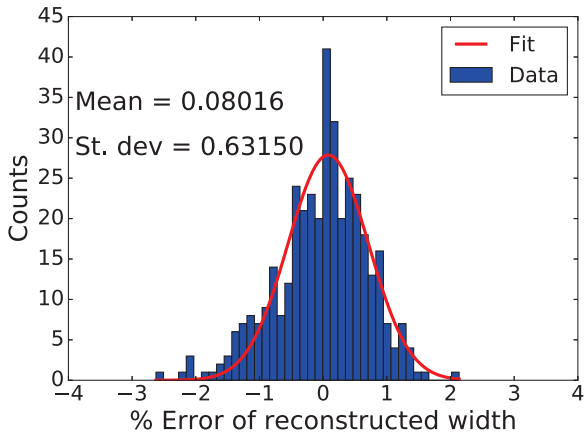

Figure 7: Histogram showing the percentage prediction error of the approximated function by the ANN-MLP.

Gaussian white noise was added to each channel on the ANN input for both training and validation data in the range of σ_{noise} = 0.5 % to 10 % relative to the maximum value to that parameter. For each set of noisy training data, the ANN training was performed 10 times and the bias and variance of prediction error was plotted against the added noise as shown in Fig. 8. A linear trend in seen in the increase of prediction error variance and bias hovers around zero. The error bar on each point denotes the variation and bias during these 10 independent runs of the training. Typical measurement uncertainties are expected to lie between 0.5-2 % in experimental scenarios.

SUMMARY

The reconstruction of distorted profiles for Gaussian beams were performed using artificial neural networks and reconstruction errors below 1 % were obtained even with the inclusion of measurement uncertainties. At this point, no good experimental data exists for the discussed case and tests with experimental data are foreseen in near future. Further, other machine learning algorithms for prediction like support vector machines will be explored and alternative instrument based training and online reconstruction of initial width from distorted profiles will be attempted.

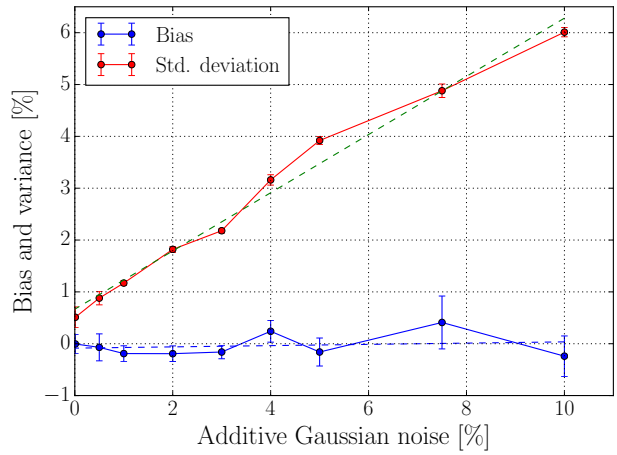

Figure 8: Evolution of bias and std. deviation of predictions with respect to noise in training and validation data.

REFERENCES

[1] R. E. Thern, "Space-charge distortion in the brookhaven ionization profile monitor", PAC 1987, Washington, D.C., USA, March 1987.

[2] Amundson *et al.*, "Calibration of the Fermilab Booster ionization profile monitor", *Phys. Rev. ST Accel. Beams*, vol.6, 102801 (2003).

[3] J. Egberts, "IFMIF-LIPAc Beam Diagnostics: Profiling and Loss Monitoring Systems", PhD thesis, University Paris Sud, (2012).

[4] M. Sapinski *et al.*, "The first experience with LHC beam gas ionization monitor", Proceedings of IBIC 2012, Tsukuba, Japan, October 2012.

[5] M. Patecki *et al.*, "Electron tracking simulations in the presence of the beam and external fields", Proceedings of IPAC 2013, Shanghai, China, June 2013.

[6] D. Vilsmeier *et al.*, "Investigation of the effect of beam space charge on electron trajectories in Ionization profile monitors", HB 2014, East Lansing, MI, USA, November 2014.

[7] D. Vilsmeier *et al.*, "A modular application for IPM simulations", IBIC 2017, Grand Rapids, MI, USA, August 2017, paper WEPCC07 , these proceedings.

[8] M. Sapinski *et al.*, "Ionization profile monitor simulations - status and future plans", Proceedings of IBIC 2016, Barcelona, Spain, September 2016.

[9] P. Forck, "Lecture notes in beam instrumentation", JUAS, 2017.

[10] K. P. Murphy, "Machine Learning: A Probabilistic Perspective", *The MIT Press*, 2012.

[11] A. Voitkiv *et al.*, "Hydrogen and helium ionization by relativistic projectiles in collisions with small momentum transfer", *J. Phys. B: At. Mol. Opt. Phys*, vol. 32, 1999.

ISBN 978-3-95450-192-2

[12] K. Hornik, "Approximation Capabilities of Multilayer Feed-forward Networks", *Neural Networks*, 4(2), 251-257, (1991).

[13] M. Abadi *et al.*, TensorFlow: Large-scale machine learning on heterogeneous systems, 2015. Software available from `https://www.tensorflow.org/`

[14] Chollet, François *et al.*, Keras, 2015. Software available at `https://github.com/fchollet/keras`

ISBN 978-3-95450-192-2